

Experimental investigation for ECC in applying to repairing water proofing structures

T. Kanda, N. Sakata, M. Hiraishi & M. Fujishiro
Kajima Technical Research Institute, Tokyo, Japan

M. Tokashiki
National Institute for Rural Engineering, Tsukuba, Japan

ABSTRACT: When joints or cracks of irrigation canals are repaired, endorsement of water tightness and crack follow-up capability for the subsequent variations in opening widths is of primary importance. Using sprayed strain hardening cement composite (hereafter denoted as ECC) expected to meet the above requirements, laboratory and full-scale experiments were performed and applicability of ECC as a repair material for irrigation canals was discussed. It was confirmed that ECC can form multiple fine cracks to accommodate variations in opening widths of cracks and joints, crack dispersion capability can be improved by introducing isolation layer and the cracks are fine enough to expect self-healing effects that greatly enhances the water tightness. Full-scale experiment has also confirmed that the variations of joint opening width can be greatly reduced when ECC is continuously applied across the joints.

1 INTRODUCTION

Strain hardening cement composite, SHCC, is a short fiber reinforced cement composite material on which worldwide active research has been conducted and particular attention has been focused in recent years. SHCC marks a strain hardening tensile stress-strain behavior like steel and exhibits excellent crack width controlling capability allowing multiple fine cracks at tensile loading (Fig. 1).

Authors have developed several applications for Engineered Cementitious Composite - ECC, a typical constituent of SHCC (Li 1993). Excellent tensile resistance and crack dispersion capability of ECC enabled various types of placement (Sakata *et al.* 2005) and sprayed ECC for repair (Sakata *et al.* 2002). These applications have been realized in repair and strengthening of existing structures such as

bridges, dams and tunnels, and further application to another types of structures is expected (Kanda *et al.* 2006).

A particular demand from irrigation canals, developed more than 40000 km in Japan, is countermeasures to damages due to surface wear-out and water leakage from joints and cracks (Fig. 2) associated with aging (Natsuka 2002). Repair of irrigation canals has been performed with a patch repair method using sprayed cement materials. However, the joints and cracks are subjected to change in opening width due to temperature variations. This leads to a premature crack and associate water leakage at early stages and degradation of the hydraulic performance (Fig. 3).

Using sprayed ECC expected to meet the above requirements, laboratory and full-scale experiments were performed and applicability of ECC as a repair

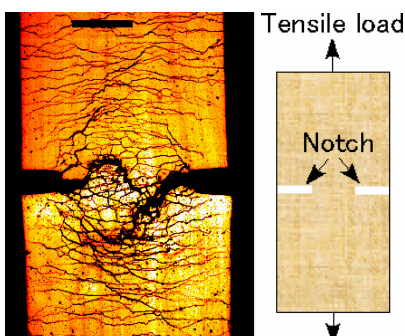


Figure 1. Crack width controlling ability of ECC (Li 1993).



Figure 2. Water leakage from joint.



Figure 3. Crack generation in repaired part.

material for irrigation canals was discussed in this study.

2 CRACK DISPERSION CAPABILITY TEST UNDER ZERO-SPAN TENSION

2.1 Objective

This test (hereafter denoted as zero-span tensile test) aimed to confirm the ECC's crack dispersion capability imitating changes in joint or crack opening width of irrigation canal.

2.2 Outline of the test

2.2.1 Specimen shape and preparation

Proposed zero-span tensile test is shown in Figure 4. Base mortar plate was made with a water to binder ratio of 0.5 and a sand binder ratio of 3.0 and reinforced with D4 steel bars. Two mortar plates are joined without a gap imitating a joint or crack of existing concrete.

Mortar plates were first treated with alumina blasting and ECC was sprayed on both sides in a dumbbell shape with a thickness of 30 mm. Specimens were subjected to sealed curing at a room temperature of 20°C and tensile test was performed

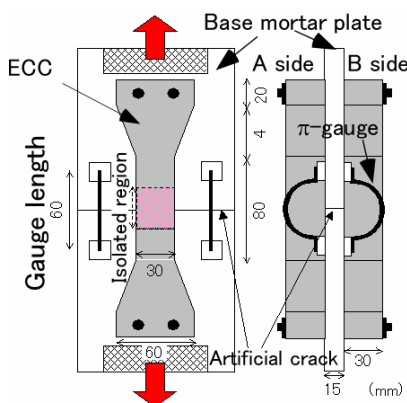


Figure 4. Zero span tensile test.

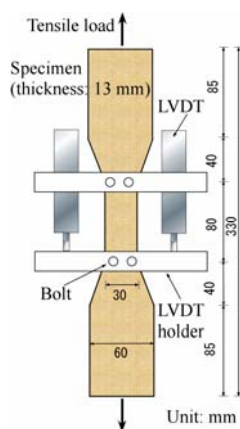


Figure 5. Uniaxial Tensile Test.

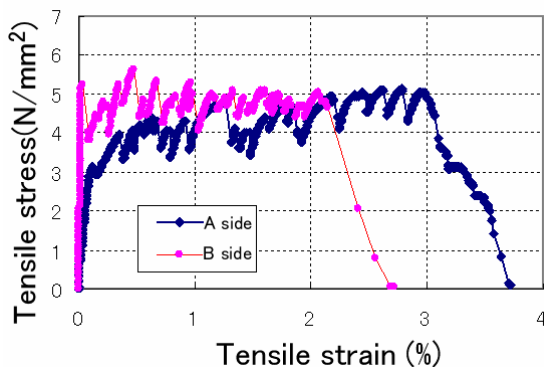


Figure 6. Tensile stress and strain relation in uniaxial tensile test.

when the age of the side A ECC was 30-day and the side B ECC was 31-day. Mix proportions of the sprayed ECC is shown in Table 1.

2.2.2 Test cases

Because effects of bond between ECC and the substrate on the crack dispersion capability of ECC should be examined, test cases were three isolation (un-bond) lengths of 0, 25 and 50 mm (hereafter denoted as case0, case25 and case50) around the model crack. The isolation region was made by masking the mortar substrate with a plastic film.

2.2.3 Testing method and test items

Specimens of zero-span tensile test were pin-supported at both ends and fixed to jigs. Tensile load was applied with displacement-controlled loading at a rate of 0.5 mm per minute to open the imitated substrate crack.

During loading, strain was measured with four pi-type strain gauges of 60 mm in length as shown in Figure 4 and the surface cracks were observed. Number of cracks and their widths at ECC surface were measured with a microscope when averaged value of two displacement transducers at both sides showed one percent (equivalent opening width of 0.6 mm). When whichever A or B sides of ECC is broken, the load was released and cracks were observed.

2.3 Result and discussion

2.3.1 Materials test

Mechanical properties of sprayed ECC and interfacial properties between ECC and substrate mortar used for the zero-span tensile test are shown in Table 2. Direct tensile testing method of dumbbell specimens is shown in Figure 5. Strain measurement gauge length was 80 mm and support of specimen was pin-fixed. Loading was applied in a displacement-controlled manner at a rate of 0.5 mm per minute. Crack opening displacement was measured when strain of the measurement length reached 1.0

Table 1. Mix proportion of ECC.

Fiber type	Fiber			Matrix		
	Fiber diameter (mm)	Fiber length (mm)	Fiber vol. Fraction (vol%)	Water to binder ratio (%)	Unit water content (kg/m ³)	Sand binder ratio
PVA	0.04	12	2	32.0	360	0.41

Table 2. ECC material testing items and results.

Test	Testing method	A side	B side
Comp. strength (N/mm ²)	JIS A 1108	46.5	38
Tensile strength (N/mm ²)	Uniaxial ensile test	5.3	5.7
Ult. Tensile strain capacity (%)		3.5	2.1
Mean crack opening disp. (mm)		0.058	—
Shear strength (N/mm ²)	Push over test (4*4*16mm)	2.3	—
Bond strength (N/mm ²)	BRI bond strength test	2.1	—

percent.

An example of stress-strain relation of single ECC is shown in Figure 6. ECC subjected to test exhibited a pseudo strain-hardening behavior that is specific to ECC, and multiple fine cracks were observed. The ultimate strain ranged from 2.0 to 3.5 percent and the mean crack opening displacement was 0.058 mm.

2.3.2 Zero-span tensile test

Two specimens per case were used for the zero-span tensile test. Some specimens were subjected to bending resulting in discrepancy in strains between side A and B. Hence the validated test results were limited to cases other than that strain of a side is smaller than a half of the strain of the other side. Specimen with the validated test result was one for each test case (two ECCs of side A and B). Results are as follows.

(1) Tensile stress-strain relations

Tensile stress-strain relations of specimens that obtained in a side ruptured first in each case are shown in Figure 7. Data immediately before rupture are shown. Pseudo strain-hardening behavior was observed for all the test cases. The strains at rupture with a test span of 60 mm were 1.29, 1.58 and 2.18 percent for case0, case25 and case50 respectively and showed larger strains at rupture with an increase in length of isolation. This can be attributed to a larger span sustaining tensile load resulting from an increase in length of isolation.

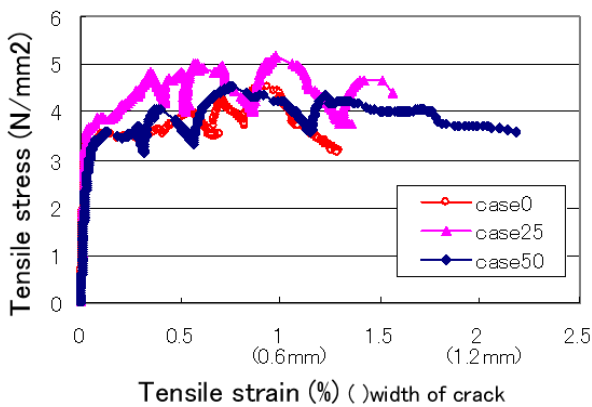


Figure 7. Stress and strain test results in zero span tensile test.

(2) Crack patterns and development

Crack patterns after test are shown in Figure 8. Cracks were observed at a wide area without limiting to the isolated region in all cases. Cracked regions spread over the isolation area and cracks dispersion capability effects were observed around the imitated crack even in zero-span case0 specimen. Specimens with isolated region were likely to show relatively larger number of cracks at isolated/non-isolated interface. This may be attributed to a shear force applied at the interface due to bond between ECC and substrate mortar.

Cracks of case0 specimen developed at the side of ECC are shown in Figure 9 where dispersed cracks form a distribution starting at the imitating crack as the apex of a triangle with an apex angle approximately 60 degree.

(3) Number of cracks and crack opening displacement

Number of cracks and crack opening displacement (COD) of ECC at both sides were measured when strain of the π -type strain gauge reached 1 percent (equivalent imitated crack opening displacement of 0.6mm) and are shown in Figure 10. Number of cracks increased and the width decreased with an increase in isolated length. In case25 and case50, the maximum crack opening displacement was smaller than 0.14 mm and almost all cracks were fine cracks with a width smaller than 0.1 mm. On the other hand in case0 specimens at zero-span condition, two large

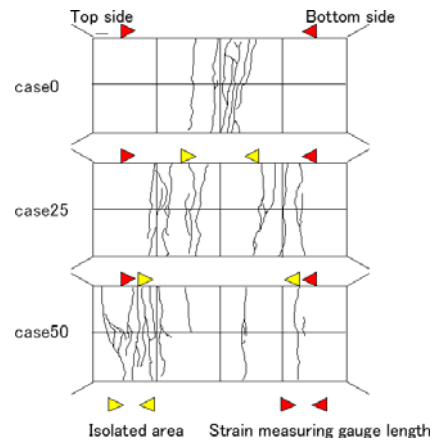


Figure 8. Crack profile on surface.

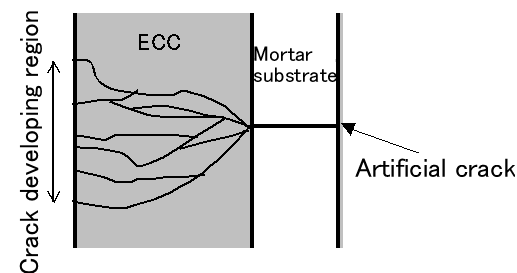


Figure 9. Crack development on edge surface.

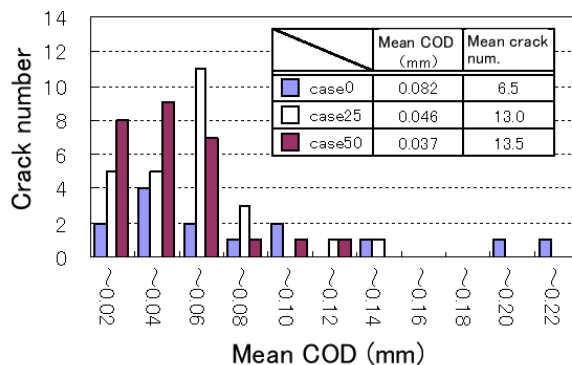


Figure 10. Frequency of crack number and mean COD.

cracks with a width larger than 0.2 mm were observed at both sides (each one at A and B side). It appeared that, at the moment, one crack was in an ultimate state of selective development, and introduction of isolation region that can increase the length for sustaining tensile load was effective in preventing localization of crack development resulting in controlling the crack opening displacement.

These test results confirm that ECC can show crack dispersion capability against variations in width of joints or cracks even at zero-span conditions while a more effective measure of improving the crack dispersion capability is to introduce a bond-isolation region between ECC and the substrate.

3 WATER PERMEABILITY TEST FOR THE CRACKED PARTS

3.1 Objectives

This test intended to verify the water tightness of ECC cracks through water permeability test for ECC and mortar with cracks.

3.2 Outline of the test

3.2.1 Specimen shape and preparation

Specimens were prepared in disk shape with dimensions of 100 mm in diameter and 15 mm in thickness. Mortar specimens were produced in casting, and ECC specimens were with spraying. Cracks in ECC specimens were introduced by splitting loading at the age of 28 days and each crack opening displacement and length were measured every 5 mm along a crack with an optical microscope. Splitting loading for ECC specimens was applied until the strain reached a specified value and the strain was monitored with a π -type strain gauge set at the center of a specimen as shown in Figure 11. Mortar specimens, on the other hand, might suffer from rupture by splitting load hence the specified crack opening displacement was

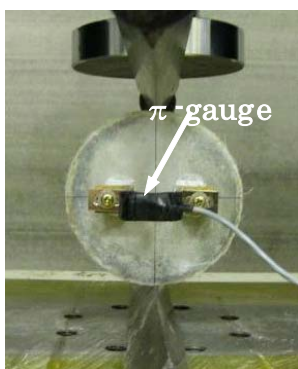


Figure 11. Testing set-up in splitting test.

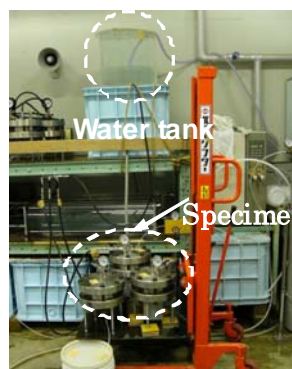


Figure 12. Water penetration splitting test.

Table 3. Outline of water permeability test.

Case	Material	Initial strain (μ)	Targeted COD (mm)
E-1000	ECC	1000	0.04
E-2000		2000	0.08
E-5000		5000	0.20
M-1000	Mortar	—	0.04
M-2000		—	0.08
M-5000		—	0.20

controlled by installing a Teflon sheet at the splitting front.

Mix proportions of the mortar and ECC were the same as employed in the chapter 2, “Crack dispersion capability test under zero-span tension”

3.2.2 Test cases

Test cases are shown in Table 3. Three different strains were introduced initially to form cracks in mortar and ECC specimens subjected to splitting test. The targeted crack opening displacement in Table 3 accounts for the length given as the product of measuring length of the π -type strain gauge of 40 mm and the initially introduced strains.

3.2.3 Testing method and test items

Execution of water permeability test is shown in Figure 12. The Output Method was adopted with an applied pressure of 15 kPa corresponding to the set-up pressure head of 1.5m. Duration was more than 24 hours until the constant flow rate was observed.

3.3 Result and discussion

3.3.1 Crack opening displacement and length

Examples of measurements for width and length of cracks before water permeability test are shown in Table 4. Number of cracks in mortar was single while that of ECC specimens such as E-2000 and E-5000 was multiple with a longer crack length than that of M-2000 and M-5000 that were prepared as control

Table 4. COD data before permeability test.

Case	Crack number	Mean COD (mm)	Crack length (mm)	Crack area (mm ²)
E-1000	1	0.023	73.1	1.7
E-2000	2	0.033	142.9	4.7
E-5000	4	0.054	214.8	11.9
M-1000	1	0.038	81.3	3.1
M-2000	1	0.08	80.9	6.3
M-5000	1	0.321	81.0	26.7

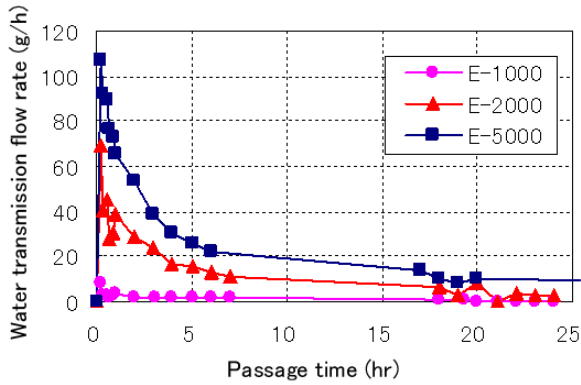


Figure 13. Water transmission amount time history in ECC.

specimens of equivalent crack opening displacement.

3.3.2 Amount of water transmission

Relationships between flow rate and passage of time for ECC and mortar specimens are shown in Figure 13 and 14. Because of the large flow rate in mortar, vertical axis of Figure 14 is exponential. As seen in

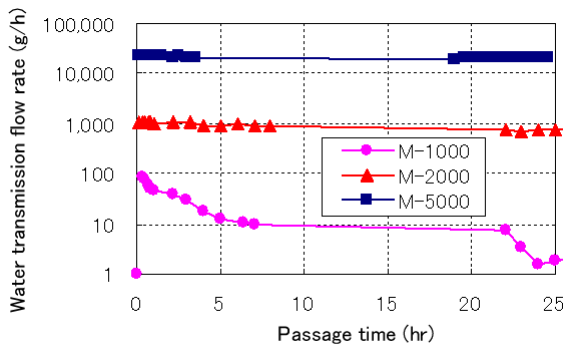


Figure 14. Water transmission amount time history in Mortar.



Figure 15. Crack opening closure after permeability test.

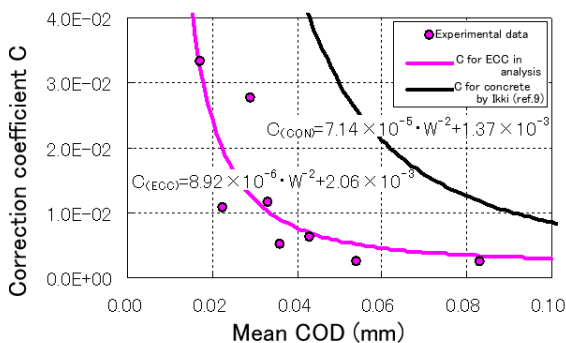


Figure 16. Effect of COD on correction coefficient C.

both figures, the flow rate of ECC is greatly reduced compared to that of mortar. This can be attributed to the crack opening displacement control capability of ECC.

Flow rates of ECC in all cases showed decrease and became constant after 24 hours while mortar specimens showed no such tendency except for M-1000 specimen that has an equivalent crack opening displacement with that of ECC. After the water permeability tests were completed, cracked part of specimens were observed and an example of ECC-5000 is shown in Figure 15 where white soluble components filled cracks. This self-healing effect was observed in all the ECC specimens. It is very likely that soluble components are easy to fill gaps in ECC capable of controlling crack opening displacement thinner, and that this effect resulted in the reduction in flow rate. The self-healing capability of ECC may be advantageous in terms of water permeability.

3.3.3 Prediction of water transfer through cracks

It is generally accepted that water flow rate through crack is proportional to the third power of crack opening displacement (JCI 2003) and given by Poiseuille's formula (Hino 1974) with a correction coefficient C that involves surface roughness of the crack and a tortuosity factor.

$$Q = C \cdot \frac{PB}{12\mu L} W^3 \quad (1)$$

where Q: water flow rate in a crack after one hour of water input (cc/s), P: water pressure (15Pa), B: crack length, μ : viscosity coefficient of water ($=1.138 \times 10^{-3}$ Pa*s), L: thickness of substrate concrete, W: crack opening displacement (cm) and C: correction coefficient.

According to Ikki *et al.* (1995), the correction coefficient C_{ECC} was calculated using the result of this experiment. The results are shown in Figure 16 together with the correction coefficient of concrete C_{CON} given by Ikki *et al.* Correction coefficient of ECC, C_{ECC} , was smaller than that of concrete, C_{CON} . This may be attributed to resistance of multiple fibers of ECC that bridge the crack interfaces even at the same crack opening displacement as that of concrete. The correction coefficient C_{ECC} obtained in this experiment showed high correlation coefficient of 0.82 with a numerical result.

It was confirmed through this experiment that ECC has an excellent water tightness even though cracks are present owing to its crack opening displacement control capability, self-healing effects and reduction in correction coefficient C originated from fiber bridging effects at crack interfaces.

4 VERIFICATION WITH AN EXISTING STRUCTURE

4.1 Objectives

Crack dispersion capability of ECC confirmed in the laboratory experiments was subjected to verification test using an existing structure for possible applicability to repair construction of joints.

4.2 Outline of the test

4.2.1 Target structure and construction method

The targeted structure was an irrigation canal built in 1979 with a unit length of 9.0 m. ECC was sprayed with a thickness of 30 mm as used in the laboratory tests. To acquire sufficient internal cross section, existing concrete was chipped for 30 mm and anchors were installed before ECC was sprayed.

4.2.2 Repair area and joint treatment

Repaired extent was 15 m including two joints and is shown in Figure 17. Joints and their neighborhoods were pretreated with silicone primer with a band of 100 mm and then the surface was treated with grease for isolation between substrate concrete and ECC, which is denoted as joint A, while that without isolation is denoted as joint B.

4.2.3 Measuring method

After construction, five pi-type strain gauges were installed at positions as shown in Figure 18 to monitor the movements of the joint. Method of measurement is shown in Figure 19. Displacements of both joint opening of substrate concrete and ECC surface were measured for joint A and B. Masking areas against ECC spray were introduced for direct bonding of pi-type strain gauge, with a measuring length of 100 mm (Con100), to measure the displacement of joint opening of substrate concrete. Another two pi-type strain gauges with measuring lengths of 100 mm and 200 mm (ECC100 and ECC200) were used to measure the displacement of ECC surfaces. For comparison, a pi-type strain gauge with a measuring length of 100 mm (Con100) was also used to measure changes in joint opening of the original concrete without ECC construction.

4.3 Result and discussion

Displacements of joint opening of concrete at North side (facing South) measured with pi-type strain gauges (Con100) and outdoor temperatures are shown in Figure 20. Assuming data obtained 14 days after construction as a control data, subsequent data are normalized and plus of minus signs are allocated to displacements in tension and in compression respectively. It is shown in Figure 20 that changes in

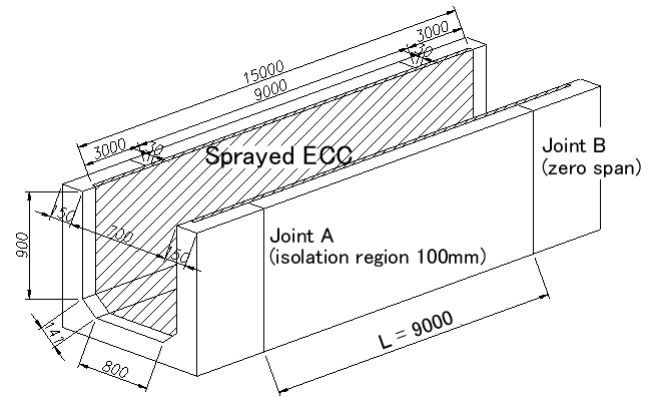


Figure 17. Existing structure and repair plan.



Figure 18. Completion of trial repair construction.

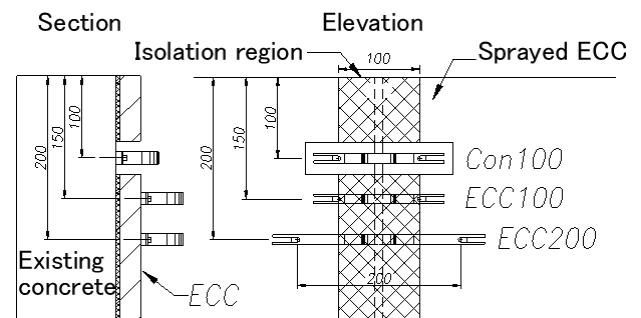


Figure 19. Measuring detail of joint movement.

joint openings are associated with changes in outdoor temperature. Variation in joint opening of concrete without ECC construction was as large as 1.8 mm while those of joint A and B with ECC construction were greatly reduced. This can be attributed to contribution of ECC that covers joints sharing tension when joint is opening and compression when closing.

Displacements of joint opening of joint A and B at North side (facing South) measured with three pi-type strain gauges are shown in Figures 21 and 22. Variation of opening in joint A with isolation region is larger than that of others. This may be, similar to the results of laboratory tests, attributed to longer span sustaining tensile stress that occurs during variations in joint opening. On the other hand, laboratory test results suggested that introduction of isolation could extend dispersion of displacement over the isolated region while measured data of Con100, ECC100 and ECC200 show no distinct differences.

After 2 months of construction, no cracks are visually observed in ECC surfaces at both joint A and B.

It is necessary for the experiments to acquire more data and discuss the validity of the isolated region.

5 CONCLUSIONS

Application of ECC spray construction for retrofitting of irrigation canals was aimed, and laboratory and full-scale experiments have been carried out. As a result, the followings are obtained.

(1) ECC showed crack dispersion capability even in a zero-span condition against variations in openings of cracks and joints. Introduction of isolation region around the opening can increase ECC's crack dispersion capability in a more effective manner.

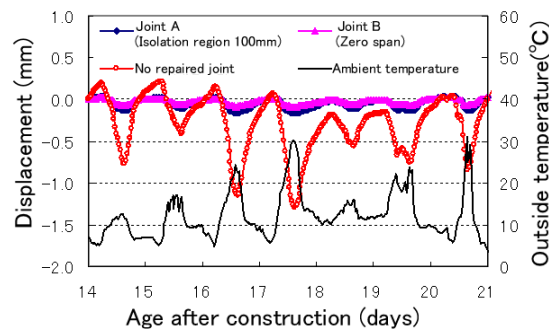
(2) Water permeability through cracks in ECC can be greatly reduced compared to that of normal concrete because ECC has a crack opening displacement controlling capability, shows reduction of correction coefficient C thanks to the resistance of fibers at crack front and has a self-healing effect.

(3) Variations in joint openings in full-scale structures can be largely controlled when ECC is applied continuously over the joints.

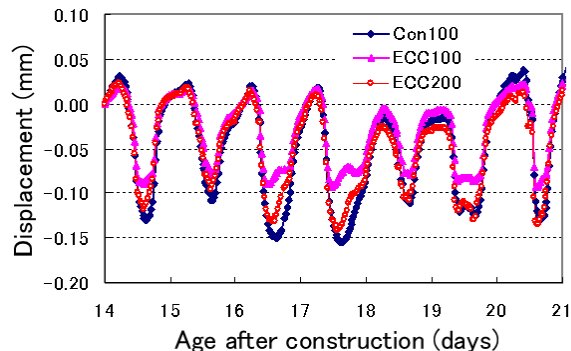
Consecutive verification tests in existing structures are needed to validate the advantage of ECC in joint constructions and optimization of ECC thickness, 30 mm at present, should be further discussed.

REFERENCES

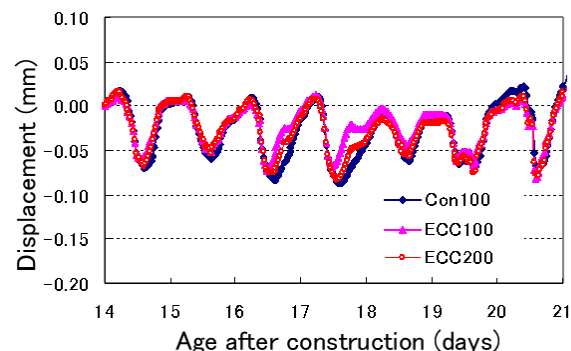
- Hino, M. 1974. Fluid mechanics, Asakura-Shoten, pp.115.
- Ikki, N., Kiyomiya, O., Yamada, M. and Takano, M. 1995. Water leakage in underground tunnel and confirmation test for the self-healing effects, *Proceedings of Japan Concrete Institute*, 17(1): 737-742.
- Japan Concrete Institute, 2003. Technical Guideline of Inspection, Repair and Strengthening of Cracks in Concrete.
- Kanda, T., Sakata, N., Kunieda, M. and Rokugo, K. 2006. State of the art of high performance fiber reinforced cement composite research and structural application, 44(3): 3-10.
- Li, V. C. 1993. From micromechanics to structural engineering-The design of cementitious composites for civil engineering applications, *Journal of Structural Mechanics and Earthquake Engineering*, JSCE, 10(2): 37-48.
- Natsuka, I. 2002. Upgrade and maintenance of irrigation and drainage concrete structures, *Journal of irrigation drainage and reclamation engineering*, 70(12): 3-6.
- Sakata, N., Suda, K. and Kanda, T. 2002. Development of spray construction system for highly ductile fiber reinforced cement composite. *Annual report, Kajima Technical Research Institute* 50: 187-190
- Sakata, N., Suda, K., Kanda, T., Fukuda, I., Hiraishi, T., Tomoe, S., Mitamura, H. and Matsui, S. 2005. Investigation for overlay reinforcement method on steel deck utilizing engineered cementitious composites, *Annual report, Kajima Technical Research Institute* 53: 221-228



Figures 20. Joint displacement time history, north side.



Figures 21. Joint displacement time history (Joint A).



Figures 22. Joint displacement time history (Joint B).